A Polyelectrolyte Brush Theory

Sanjay Misra* and Sasidhar Varanasi

Department of Chemical Engineering, The University of Toledo, 2801 W. Bancroft, Toledo, Ohio 43606

P. P. Varanasi

S. C. Johnson & Son Inc., Racine, Wisconsin 53403. *Received January 19, 1989; Revised Manuscript Received April 14, 1989*

ABSTRACT: The self-consistent-field (SCF) polymer brush theory of Milner–Witten–Cates is extended to the case of a polyelectrolyte brush, along the lines of earlier polyelectrolyte adsorption theories. This is accomplished by equating the sum of the electrostatic and nonelectrostatic potential fields to an overall parabolic potential; the conditions of validity of such a parabolic variation of the overall potential distribution have recently been established by Milner et al. Chains of segment length 1000 with a segment size of 1 nm are considered in a moderately good solvent (χ = 0.45). The effects of brush charge, indifferent electrolyte concentration, surface charge, and grafting density (σ) on the segment density profiles, brush height, and free energy of polyelectrolyte brush are explored. The segment density profiles are observed to deviate from the parabolic shape with increasing brush charge and lower ionic strengths. While the brush height scales as $\sigma^{1/3}$ for nonionic brushes, the exponent shows significant deviations from 1/3 for polyelectrolyte brushes with decreasing ionic strength. The scaling exponent for free energy, however, shows no significant deviation from its value of 2/3 for the nonionic brush.

1. Introduction

The properties of polymers at interfaces are of considerable interest in the area of steric stabilization of colloids.[1-3] Charged polymers (polyelectrolytes) are also useful for selective flocculation of ores and for modifying the ion-exchange capabilities of the adsorbents.[4] One very important application of a polyelectrolyte interface could be to change the permeability of porous media and make the permeability pH sensitive. It has been shown that polyelectrolyte adsorption in porous membranes could make their permeability characteristics pH sensitive.[5,6] Indeed, as suggested by Idol and Anderson,[6] by suitable tailoring of polymeric molecules one can improve the selectivity of an otherwise nonselective membrane.

Polymer brushes are formed by grafting polymer chains terminally to the surface, in high density. One method of accomplishing this is by the adsorption of macromolecular amphiphiles (diblock copolymers), one block of which would show a high affinity for the surface, assuming a flat configuration next to the adsorbing surface. The other block, on the other hand, would have no affinity for the surface and would stretch away from the surface into the solvent. Brushes formed by such diblock copolymer adsorption offer definite advantages over the adsorption of homopolymers.[1] Any bridging, in the case of colloid stabilization, would be precluded since the chains extending from one surface would have no affinity for the other surface. Also, since the bonds between the binding polymer block and the adsorbing surface are very strong, desorption of the adsorbed block would not occur easily, and the interface would retain its properties almost indefinitely. In the case of membrane permeability, it would mean that the alteration in the membrane properties would be made permanent by grafting a polyelectrolyte brush within the pores.

The properties of polymers in solution and at interfaces have been the subject of much investigation. Various approaches to describing the configuration of terminally attached nonionic polymer chains have been used.

Using Flory arguments of global energy balance and scaling principles, Alexander[7] and de Gennes[8,9] concluded that in the adsorbed brushes the polymer chains are highly stretched and that the segment density distribution (SDD) in the brush layer is uniform for almost the entire length of the brush.

The self-consistent-field (SCF) approach provides a powerful tool for the study of polymer chain conformations. In this approach, no a priori assumptions are made for the segment density distribution of the polymer chains. The distribution arises by solving the field equation in which the potential field acting on each segment depends upon the density distribution itself. A *lattice* version of this approach, developed by Scheutjens and Fleer[10] for homopolymer adsorption, has been utilized by Cosgrove et al.[11] and by Hirz[19] for describing terminally attached chain configurations as well. The segment density distributions obtained by Cosgrove et al. and by Hirz, however, differ from the uniform segment density predicted by scaling analysis.

The self-consistent-field (SCF) approaches in *continuum* have been used extensively for describing the configuration of homopolymers by Edwards, de Gennes, Dolan and Edwards, Helfand, Richmond and Jones, and Polehn et al.[12-18] It has been pointed out by early investigators[12,13] that there exists a strong analogy between configurations of flexible polymer chains and the paths of quantum-mechanical particles. Recently, Milner et al.[19] have described the properties of a grafted brush using the SCF approach in continuum. However unlike many other studies employing continuous space SCF formalism, which focus on the situations where the physics of the system is dominated by the so-called "ground-state" solution of the relevant SCF (Schroedinger) equation, Milner et al. solve the SCF equation in its "classical limit" (after delineating the conditions under which the partition function of the brush is dominated by the classical paths of the polymer chains). Specifically, they have established, under the conditions leading to brush formation, an analogy between the conformation of a polymer chain and the path of a *Newtonian* particle of unit mass moving under the influence of a potential field. Further, assuming that all the grafted chains are of equal length, they have shown that, within the brush, the potential variation with the distance from the grafting surface is parabolic. This is quite an elegant and surprisingly simple result. In the cases where the segment density is not too high, it is shown by Milner et al. that the segment density distribution itself is parabolic. This

* Author to whom correspondence should be addressed.

0024-9297/89/2222-4173$01.50/0

result compares extremely well with the lattice theory based computations of Hirz and those of Cosgrove et al. (for the larger chain length of 250) but is at variance with the uniform segment density prediction of Alexander and de Gennes. However, the predictions of Milner et al. for the scaling of brush height and free energy with chain length and coverage do coincide with those of Alexander and de Gennes.

Experimental data on brush conformations are not extensively available as yet. Studies, however, have been performed recently on force measurements between surfaces with adsorbed diblock copolymers[20,21] and on hydrodynamic permeability of membranes with adsorbed diblock copolymers inside the pores.[22]

In this work, the brush theory of Milner et al. is extended to the case of a polyelectrolyte brush formed on a charged planar substrate immersed in an aqueous solution of a Z:Z electrolyte. The approach is based on expressing the total potential acting on the segments as the sum of the nonelectrostatic potential arising from the nonionic segment–segment and segment–solvent interactions and the electrostatic potential arising due to the charges on the substrate and on the segments. The total potential itself, however, remains parabolic as long as the conditions for the chain configuration–particle path analogy of Milner et al. are met and the chains are all of equal length. These conditions are discussed in the next section. The effects of brush charge, indifferent electrolyte concentration, surface charge and coverage on segment density, brush height, and free energy per chain are studied. A similar approach by Miklavic and Marcelja[23] was brought to our notice by one the referees. Their work is compared to the present effort in section 5.

The organization of this paper is as follows. In the following section, those aspects of the polymer brush theory of Milner et al. that are relevant to the present work are briefly recapitulated. In section 3, the governing equations for extending the nonionic polymer brush theory to polyelectrolyte brushes are presented. This is followed by a brief outline of a numerical scheme for solving these equations in section 4. Finally, some results specific to polyelectrolyte brushes, obtained from the above model, are presented and discussed in the light of the predictions for nonionic brushes.

2. Theory of Grafted Brushes

First, the conditions under which terminally attached chains form a "brush" are reviewed as delineated by Alexander and de Gennes. Subsequently, a brief description of those aspects of Milner et al.'s brush theory[19] pertinent to the present work and the conditions under which the latter theory is valid are given.

As pointed out by Alexander,[7] the spacing between the grafting points, D, is the important parameter that determines the conformation of the terminally attached chains. If D is of the order of, or greater than, the radius of gyration, R_g, of free polymer chains, the grafted chains assume configurations resembling adjacent "mushrooms". On the other hand, if $D < R_g$, the polymer chains stretch out into the solution, due to excluded volume interactions, forming a brush. de Gennes[9] points out that in this regime the chains build up a region of uniform segment concentration, whose thickness is given as

$$h^* = Na(a/D)^{2/3} \tag{1}$$

where h^* is the overall thickness of the brush, a is the segment size, and N is the number of segments in the chains. The brush height h^* thus scales as $\sim ND^{-2/3}$. de Gennes,[9] however, also notes that, while the SDD remains uniform throughout the brush height, there exist two end zones of approximate length D one next to the wall and one at the the other end of the brush, where the segment density drops from the uniform value. In the zone near the wall, the density drops due to the segment–wall interactions (and entropic repulsions) in a power law fashion; at the other end, the segment density decays exponentially to zero.[9,20]

Turning to Milner et al.'s model, these authors used, as mentioned in the Introduction, a self-consistent-field approach to describe the properties of the grafted brush. Their model brings out in an explicit manner the analogy between the configurations of the grafted chains and the trajectories of particles in a potential field, which permits them to obtain an elegant solution to the field equations. These authors exploit the insight provided by the theories of Alexander and de Gennes that the chains in a brush are strongly stretched (i.e., $h^* \sim N$, see eq 1). Therefore, for long chains $h^* \gg R_g$ ($\sim N^{1/2}$). Under these conditions, the fluctuations of a grafted chain about its average configuration become unimportant (as their amplitude is $\sim R_g$). This observation is also supported by the lattice-based calculations of Cosgrove et al.,[11] who show that with increasing chain length the fraction of segments bound to the adsorbing surface drops off and the chains are more and more stretched in the form of tails. This allows one to determine the brush properties (viz. h^*, SDD, free energy of the brush, etc.) on the basis of the average (or classical) configurations only. The problem is thus simplified since one has to account only for the classical paths of the chains instead of taking into account all paths, which would warrant the solution to the SCF equation involving the quantum-mechanical propagator, G (see ref 12 and 13 for further details). As alluded to in the Introduction, the SCF approach requires a scheme to relate the potential field acting on a segment to the detailed structure of its environment. Milner et al. employ the so called mean-field approximation for this purpose; i.e., each segment interacts with all others only through an average concentration of segments. Such a mean-field approximation is valid when the grafting density is sufficiently high and the solvent quality is not too good. The latter requirement ensures that the chains do not repel each other strongly and the segment density does not become too low due to brush swelling. Milner et al. also assume that segment–wall interactions are absent. This assumption does not constitute a serious limitation since, according to de Gennes, under conditions leading to brush formation the segment–wall interactions are confined to a small length D. (See also Figure 4, ref 11.) These key observations form the basis for their analysis.

The conformation of the ith chains may be represented by a set of N position vectors $\mathbf{r}_i(n)$, where n (which assumes values 1 to N) represents the rank of the segment. The rank of the grafted segment of the chain is N, and its x coordinate is $x_i(N) = 0$, x being the direction normal to the wall. Considering that under strong stretch conditions the single-chain partition function is dominated by classical paths, one can neglect the contribution of nonclassical paths to the partition function. Milner et al. conclude that the change in free energy ΔF_i upon removing one chain (or the logarithm of the single-chain partition function), keeping the others fixed, is given by

$$\Delta F_i = \frac{1}{2}\int \mathrm{d}n \left(\frac{\mathrm{d}\mathbf{r}_i}{\mathrm{d}n}\right)^2 + \int \mathrm{d}n \, \frac{\partial F}{\partial \Phi}[\mathbf{r}_i(n)] \tag{2}$$

In eq 2, only the maximum term of the partition function is retained, corresponding to the classical paths of the

chains. The deviations around the classical paths are, as noted earlier, negligible, and hence the other terms in the partition function are unimportant. Here F is the free energy of the chains in the brush and Φ is the local segment volume fraction. The first term in eq 2 corresponds to the stretch free energy and the second to the excluded volume energy. This representation for the stretch free energy, as pointed out by Milner et al., breaks down when the brush length approaches the length of fully stretched molecules, since it is derived for the case of low orientational order.[13] (For a further understanding of the "energy-integral" of eq 2, see ref 13 and 19.)

Using the mean-field approximation, one can substitute for the effective potential

$$U(\mathbf{r}) = -(\partial F/\partial \Phi) \tag{3}$$

With this substitution, eq 2, as pointed out by Milner et al., corresponds to the path integral for one particle classical mechanics in potential $U(\mathbf{r})$. The stretch energy corresponding to the kinetic energy of a particle whose position at "time" in (where $i = (-1)^{1/2}$) is given as $\mathbf{r}_i(n)$.

In the classical limit of highly stretched chains, ΔF_i is minimized with respect to the path $\mathbf{r}_i(n)$, to obtain the equation describing those paths that dominate the physics of the brush. All other paths are neglected. This is done by fixing each chain end and varying the path of the rest of the chain to obtain

$$d^2\mathbf{r}_i/dn^2 = -\nabla_r U(\mathbf{r}) \tag{4}$$

The above equation is analogous to the equation of motion of a classical particle in a potential $U(\mathbf{r})$.

As the second step, one varies the position of the free end of a chain, ρ_i, while the conformation of the chain satisfies eq 4.

$$\frac{\partial \Delta F(\rho_i, \mathbf{r}_i(n))}{\partial \rho_i} = 0; \quad \rho_i = \mathbf{r}_i(0) \tag{5}$$

Thus, at equilibrium eq 5 (implying minimum free energy of system) will be satisfied subject to eq 4 (describing the conformation of the chains).

At the free end of the molecules, ρ_i, the stretching rate is zero since the chains are in mechanical equilibrium or

$$\left(\frac{d\mathbf{r}_i}{dn}\right)\Bigg|_{\rho_i} = 0 \tag{6}$$

Having established the analogy between a particle trajectory in potential $U(\mathbf{r})$ and the conformation of a chain, Milner et al. then exploit the monodispersity of the chain length of the macromolecules.

All the particles start at some distance (corresponding to x (ρ_i)) from the walls with a zero velocity (see eq 6) and fall toward the wall under the influence of the potential $U(\mathbf{r})$. However, since all chains are the same length, the "time" taken for these particles to reach the wall is the same. This would imply the potential of a harmonic oscillator in the brush, with each particle executing one quarter cycle of its oscillation. In this case, the potential is one dimensional, so that $U(\mathbf{r}) \equiv U(x)$ and is given by an expression of the form

$$-U(x) = A - Bx^2 \tag{7}$$

where $B = \pi^2/8N^2$. The constant A is determined by a mass balance to ensure that the total amount of material in the brush equals the total amount of material grafted. The authors show that an expression of the type $U = -\omega\Phi$, where ω is the excluded volume parameter, leads to a segment volume fraction profile of the form

$$\Phi(x) = \omega^{-1}(A(h) - Bx^2)$$

$$A(h) = \frac{N\sigma\omega}{h} + \frac{Bh^2}{3} \tag{8}$$

where σ is the surface density of the grafted chains and h is the brush height. The brush height under no external forces is found as $h^* = (12/\pi^2)^{1/3}(\sigma\omega)^{1/3}N$. The brush height scales as $\sim N\sigma^{1/3}$. Also, since $\sigma \sim D^{-2}$, Milner et al.'s theory predicts a brush height that scales as $\sim ND^{-2/3}$. This is in complete agreement with the scaling predictions of Alexander and de Gennes.

3. Extension to Polyelectrolyte Brushes

If the conditions for the SCF theory outlined in the previous section are satisfied, then one can extend the equal time argument for monodisperse chains to the case of polyelectrolyte brushes as well. The extension of the brush theory to polyelectrolytes is along the lines of Hesselink,[4] Papenhuijzen et al.,[24] and Van der Schee and Lyklema,[25] who have extended for polyelectrolytes the polymer adsorption theories of Hoeve,[26] Roe,[27] and Scheutjens and Fleer[10] and Roe,[27] respectively. As in the case of these theories, the total free energy of the system (F) is equated to the sum of the electrostatic (F_E) and nonelectrostatic (F_N) parts:

$$F = F_N + F_E \tag{9}$$

Since the total potential $U(x) = -\partial F/\partial \Phi$ (see eq 3), we have

$$-U(x) = \frac{\partial F}{\partial \Phi} \equiv \frac{\partial F_N}{\partial \Phi} + \frac{\partial F_E}{\partial \Phi} \equiv -U_N(x) - U_E(x) \tag{10}$$

where $U_N(x)$ and $U_E(x)$ represent the nonelectrostatic and electrostatic components of the total potential, respectively.

Using the Flory solution theory for the free energy, F_N, one obtains the following expression for U_N,[18] which is valid for a wider range of segment concentrations compared to the expression employed by Milner et al.:

$$-\frac{U_N}{kT} = -\ln(1 - \Phi) - 2\chi\Phi \tag{11}$$

The electrostatic part, U_E, of the total potential is given as[24]

$$-\frac{U_E}{kT} = \frac{fZ_s e\Psi}{kT} \tag{12}$$

where Ψ is the electrostatic potential, f is the average degree of charging of the segments, Z_s is the valence of the segments, and e is the protonic charge. All segments are assumed to be equally dissociated in this model, irrespective of their spatial position in the brush, which makes f independent of x in the model.

Since the potential is parabolic, using eq 10, 11, and 12, one can write

$$\alpha - \beta t^2 = -\ln(1 - \Phi) - 2\chi\Phi - ru \tag{13}$$

Here a nondimensional length scale, t, is used by scaling down x with a factor of κ^{-1}, the Debye screening length (defined later). Thus $t = \kappa x$. u is the dimensionless potential $Ze\Psi/kT$, where Z is the valence of the cation of the symmetrical electrolyte considered here. Thus, $r = -fZ_s/Z$. Taking the "time" coordinate as the contour length ($=na$), instead of the segment ranking ($=n$) as done by Milner et al., one obtains $\beta = \pi^2/(8N^2a^2\kappa^2)$, which is the dimensionless version of the constant B defined by Milner et al. in eq 7. α is the dimensionless total potential of a segment located next to the wall, which can be determined as explained in section 4.

To obtain the segment density profile, one has to solve the Poisson equation. This equation has to be solved for two regions: the inner or the brush region, which includes the fixed charges due to the polyelectrolyte in addition to the mobile ions of the electrolyte, and an outer region, where only the mobile ions of the electrolyte are present. The Poisson equation, assuming Boltzmann distribution for the mobile ions, takes the following form for the inner and outer regions, respectively:

$$\frac{d^2\Psi^{(i)}}{dx^2} = -\frac{4\pi}{\epsilon}\left[-2n_\infty Ze \sinh\left(\frac{Ze}{kT}\Psi^{(i)}\right) + \frac{fZ_s e}{\nu_s}\Phi\right]; \quad 0 \le x \le h_1^* \tag{14}$$

For the outer layer one has

$$\frac{d^2\Psi^{(o)}}{dx^2} = -\frac{4\pi}{\epsilon}\left[-2n_\infty Ze \sinh\left(\frac{Ze}{kT}\Psi^{(o)}\right)\right]; \quad h_1^* < x \le \infty \tag{15}$$

Here n_∞ is the bulk electrolyte concentration, h_1^* is the equilibrium brush height of the *polyelectrolyte* brush, and ν_s is the segment volume. The superscripts (i) and (o) refer to the inside and outside layers, respectively. Substituting $u = Ze\Psi/kT$ and defining $\kappa^{-1} = [\epsilon kT/(8\pi Z^2e^2n_\infty)]^{1/2}$, one has, for the inner (or brush layer)

$$\frac{d^2u^{(i)}}{dt^2} = \sinh(u^{(i)}) + \frac{r}{2n_\infty\nu_s}\Phi; \quad 0 \le t \le t^* \tag{16}$$

and for the outer layer

$$\frac{d^2u^{(o)}}{dt^2} = \sinh(u^{(o)}); \quad t^* < t \le \infty \tag{17}$$

where $t^* = \kappa h_1^*$.

$u^{(i)}$ and $u^{(o)}$ satisfy the following boundary conditions:

$$\text{at } t = 0, \quad \frac{du^{(i)}}{dt} = -\frac{\kappa\sigma_0}{2Zen_\infty} \tag{18}$$

$$\text{as } t \to \infty, \quad u^{(o)} \to 0 \tag{19}$$

where σ_0 is the total surface charge density on the adsorbing plane.

Equations 16 and 17 are solved for the electrostatic potential distribution within and outside the brush region, respectively, and the solutions are matched by requiring that the electrostatic potential and its derivative be continuous at $t = t^*$. In other words

$$u^{(i)}(t=t^*) = u^{(o)}(t=t^*) \tag{20}$$

$$\frac{du^{(i)}}{dt}(t=t^*) = \frac{du^{(o)}}{dt}(t=t^*) \tag{21}$$

The solution of the Poisson–Boltzmann equation within the brush region requires knowledge of Φ, the segment density distribution, which is yet to be determined. However, since the potential in the outer layer, $u^{(o)}$, does not require knowledge of Φ, its solution can be readily written in the following analytical form by using the Guoy–Chapman theory:

$$\tanh\left(\frac{u^{(o)}}{4}\right) = \tanh\left[\frac{u^{(o)}(t=t^*)}{4}\right]e^{-(t-t^*)} \tag{22}$$

Using equations of continuity 20 and 21 and eq 22, one can write

$$\text{at } t=t^*, \quad \frac{du^{(i)}}{dt} = -2\sinh\left(\frac{u^{(i)}}{2}\right) \tag{23}$$

Since both the boundary conditions on u for the brush region have been established in the form of eq 18 and 23, one can now solve the Poisson–Boltzmann equation exclusively within the brush along with eq 13. Equation 13 is differentiated with respect to t and solved simultaneously with eq 16 for the segment and electrostatic potential profile. Substituting $Y_1 = \Phi$, $Y_2 = u^{(i)}$, and $Y_3 = du^{(i)}/dt$, one obtains the following three governing first-order ordinary differential equations:

$$\frac{dY_1}{dt} = \frac{rY_3 - 2\beta t}{(1 - Y_1)^{-1} - 2\chi} \tag{24}$$

This equation is obtained by the differentiation of eq 13. Equation 16 can be written as two first-order equations as follows:

$$\frac{dY_2}{dt} = Y_3 \tag{25}$$

$$\frac{dY_3}{dt} = \sinh Y_2 + \frac{r}{2n_\infty\nu_s}Y_1 \tag{26}$$

The segment density is required to vanish at the brush height, giving us the boundary condition

$$t = t^*, \quad Y_1 = 0 \tag{27}$$

The boundary conditions given in eq 18 and 23 can be rewritten as

$$t = 0, \quad Y_3 = -\kappa\sigma_0/(2Zen_\infty) \tag{28}$$

$$t = t^*, \quad Y_3 = -2\sinh(Y_2/2) \tag{29}$$

respectively. Solution of the above governing equations, eq 24–26, requires knowledge of t^*, which appears in the boundary conditions (eq 27 and 29). The value of t^* is determined by requiring it to satisfy the constraint that the number of segments contained in the brush volume per unit area of the wall equals $N\sigma$.

$$\sigma N\nu_s = (1/\kappa)\int_0^{t^*} dt\ \Phi(t) \tag{30}$$

Equations 24–30 form the complete formulation for the polyelectrolyte brush problem. The simultaneous solution of these equations yields the segment density profile.

4. Segment Density Distribution and Free Energy

Equations 24–30 represent a problem of solving a set of nonlinear ordinary differential equations with boundary conditions at two different points. The position of the end point $t = t^*$ itself is not known at the outset. To begin with, an initial estimate was made for t^* by using eq 8, where ω was substituted by $1 - 2\chi$. With this t^*, eq 24–29 were solved by using a finite difference technique to obtain the segment density distrubition, $\Phi(t)$. In this case the IMSL subroutine BVPFD was employed to solve the set of differential equations. The density profile, $\Phi(t)$, was integrated to check whether it satisfied eq 30. The normalized error was defined, on the basis of eq 30, as

$$\Delta^{(k)} = \frac{\int_0^{t^{*(k)}} dt\ \Phi^{(k)}(t) - \sigma N\nu_s\kappa}{\sigma N\nu_s\kappa} \tag{31}$$

where the superscript (k) denotes the solution at the kth iteration. Subsequent values of t^* were then determined by using the Regula–Falsi method. An interactive scheme using eq 31 and the Regula–Falsi method was set up to solve eq 24–29 until convergence was reached, i.e., when eq 30 was satisfied within some tolerance limit. The

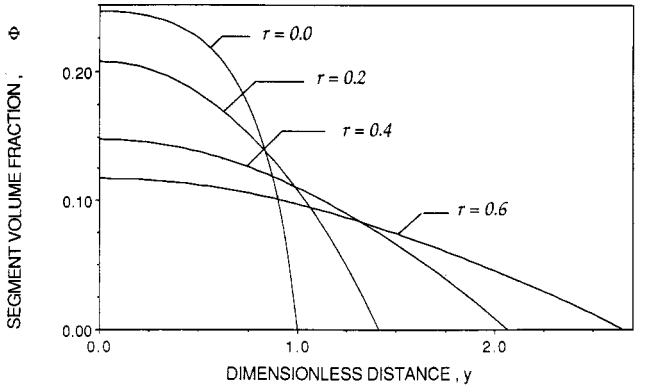

Figure 1. Effect of brush charging r on the segment density distribution: 1:1 electrolyte at 0.1 M ionic strength, $\chi = 0.45$, surface charge $\sigma_0 = 0.0$, $\sigma = 10^{17}$ m^{-2}, $N = 1000$, $a = 1 \times 10^{-9}$ m.

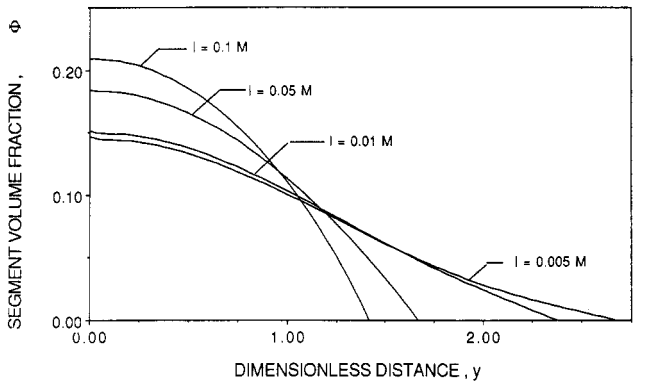

Figure 2. Effect of ionic strength I on the segment density distribution: 1:1 electrolyte, $r = 0.2$, $\chi = 0.45$, surface charge $\sigma_0 = 0.0$, $\sigma = 10^{17}$ m^{-2}, $N = 1000$, $a = 1 \times 10^{-9}$ m.

Regula–Falsi method converged rapidly and satisfactorily to the final value of t^*. The value of α, the dimensionless potential of a segment next to the wall, can now be determined by substituting the known profiles for $u^{(i)}$ and Φ in eq 13.

One can now use the computed values of α to do further computations for brush free energy. The free energy per chain, $\mathcal{F}$, is calculated (as discussed by Milner et al.) as

$$\frac{\mathcal{F}}{kT} = \frac{N}{\sigma}\int_0^{\sigma} d\sigma'\, \alpha(\sigma') \qquad (32)$$

5. Results and Discussion

In the figures we discuss next, the effect of some important variables on the segment density distribution is illustrated. The effects of r (the degree of segment charging), n_∞ (the bulk electrolyte concentration), and $\sigma' = \sigma_0\kappa/(2Zen_\infty)$ (the dimensionless surface charge) are considered. Chains of $N = 1000$ segment length with a segment size of $a = 1$ nm are assumed. A 1:1 electrolyte, in water at 298 K, is considered. The segment volume is calculated as $\nu_s = (\pi/6)a^3 = 5.236 \times 10^{-28}$ m^3. In Figures 1–4, discussed below, the dimensionless distance from the surface, y, is the ratio of the actual distance from the surface, x, to the height of a free uncharged polymer brush, h^*; i.e., $y = (x/h^*)$. Here h^* was determined to be 2.62×10^{-7} m, for $\sigma = 1 \times 10^{17}$ m^{-2}. The radius of gyration, R_g, of the (random freely jointed) chain is $\sim 1.3 \times 10^{-8}$ m or $h^*/R_g \sim 20$. This satisfies the strong stretch condition, yet h^* is only 26% of the length of totally stretched chain. Hence the stretch free energy representation is satisfied. In all four figures, h^* never exceeds about 70% of the fully stretched chain (or $y^* \leq 2.6$), and the stretch representation could be considered as a satisfactory approximation under the conditions explored in the figures.

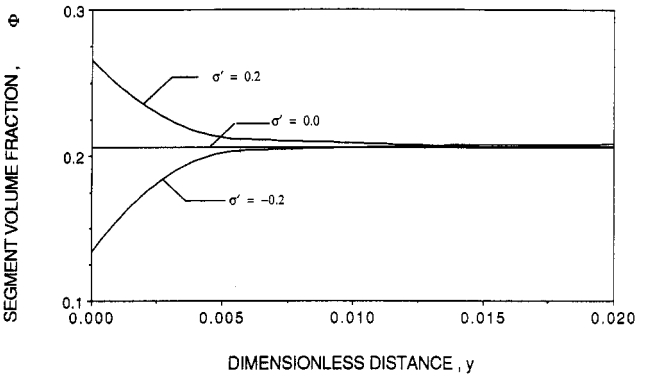

Figure 3. Effect of surface charge σ_0 on the segment density distribution: $r = 0.2$, 1:1 electrolyte at 0.1 M ionic strength, $\chi = 0.45$, $\sigma = 10^{17}$ m^{-2}, $\sigma' = \sigma_0\kappa/(2Zen_\infty)$, $N = 1000$, $a = 1 \times 10^{-9}$ m.

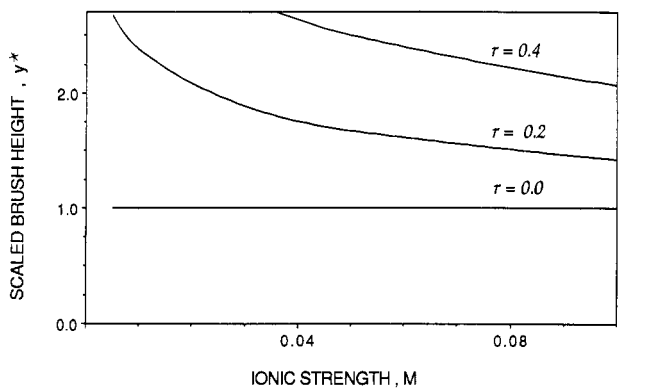

Figure 4. Effect of ionic strength I on the brush height y^*: $\chi = 0.45$, surface charge $\sigma_0 = 0.0$, $\sigma = 10^{17}$ m^2, $N = 1000$, $a = 1 \times 10^{-9}$ m.

As illustrated by Figure 1, the brush height increased with increasing r, or brush charge. This is expected since with an increasingly charged brush the repulsion among the segments would become stronger, forcing the macromolecules to stretch further and further. This causes the brush to swell. If the brush-forming chains were weak polyelectrolytes, their dissociation and hence the brush charge could be controlled by pH variation.

In Figure 2, the effect of bulk electrolyte concentration is explored. It is noticed that with increasing electrolyte concentration the brush height decreases. This is not an unexpected result since with increasing electrolyte concentration the electrostatic potential decays quickly, allowing the chains to concentrate closer to the surface. At low electrolyte concentrations, the brush charges are not screened effectively, leading to the swelling of the brush layer (analogous to nonionic brush swelling in good solvents) through repulsion between segments.

The surface charge predominantly affects the density profile near the surface. Since the Debye screening length is a small fraction of the overall brush height, the effect of surface charge is limited to a small region of the brush, and the density profile away from the surface is not significantly affected by all but very high values of surface charge. Even in the presence of an opposite surface charge, the strong stretching assumption is not violated since the attraction of the chains to the surface is far outweighed by electrostatic and excluded volume repulsions. This is illustrated in Figure 3.

Figure 4 demonstrates the effect of ionic strength on the brush height for various values of r. As noted earlier, increased ionic strength leads to better screening of polyelectrolyte charges and less intersegmental repulsions. As expected, the brush height approaches the uncharged brush height with increasing ionic strength. Thus the

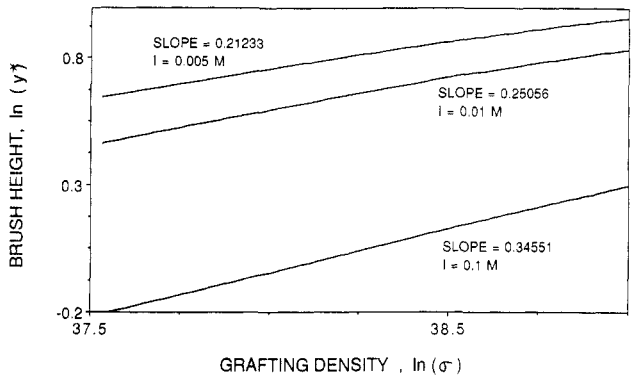

Figure 5. Effect of ionic strength I on the scaling of brush height y^* with D: $r = 0.2$, $\chi = 0.45$, surface charge $\sigma_0 = 0.0$, $N = 1000$, $a = 1 \times 10^{-9}$ m.

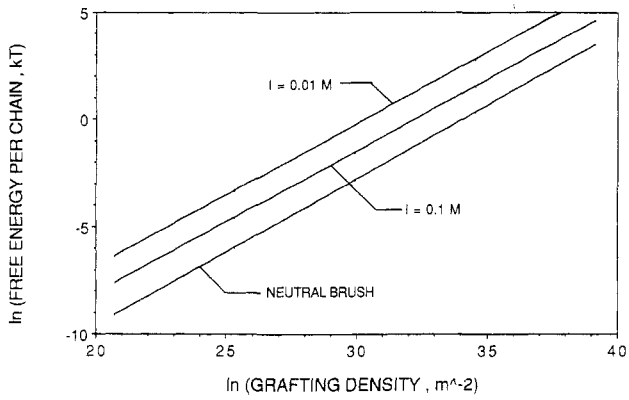

Figure 6. Effect of ionic strength I on the variation of free energy per chain $\mathcal{F}$ with D: $r = 0.2$, $\chi = 0.45$, surface charge $\sigma_0 = 0.0$, $N = 1000$, $a = 1 \times 10^{-9}$ m.

behavior of the polyelectrolyte brush approaches that of uncharged brushes with high ionic strengths.

In Figure 5, the grafting density was varied between 2×10^{16} and 1×10^{17} m^{-2}. The objective was to determine, in that range of grafting density, the effect of ionic strength on the scaling structure of the brush height with the average spacing of grafting points, D. As noted earlier, the theories of Alexander, de Gennes, and Milner et al. predict that h^* scales as $D^{-2/3}$. As illustrated in Figure 5, the scaling exponent deviated more and more from the value of $-2/3$ as ionic strength decreased and the electrostatic repulsions between the segments became stronger. With higher ionic strengths, the electrostatic repulsions between the chains were screened more effectively, and the behavior of the brush approached that of a nonionic brush. The scaling exponent under these conditions approached a value of $-2/3$.

In Figure 6, the free energy, per chain of the brush, is computed for different ionic strengths and compared with that of a similar uncharged brush. The free energy increases by orders of magnitude for ionic brushes, especially as the ionic strength gets lower. This is not surprising since the electrostatic work to bring a chain to an already charged environment is very high compared with the excluded volume interaction, which operates only at short ranges. With lowered ionic strength, the charges are not effectively screened, and hence the free energy increases due to greater intersegmental repulsions. In the range of the parameters investigated in Figure 6, the free energy scales with grafting density in the same manner irrespective of the ionic strength and the scaling exponent (the slope of the line), at all ionic strengths, is the same as that for a nonionic brush. This is a surprising result since the scaling exponent for the brush height varies significantly under the same change in ionic strength.

It is fair to point out (see also ref 24) that the use of the mean-field approximation is valid only at sufficiently high segment concentrations (or sufficient coil overlap), where the segments can be assumed to interact with each other and with the solvent through an average local concentrations; self-avoidance is not an important consideration. However, with low grafting density, increasingly charged brushes, or low ionic strengths, the brushes would tend to swell, leading to lowering of segment concentrations. At higher ionic strengths or lower segment charging (analogous to an only moderately good solvent), though, one could approach the results of this theory with more confidence.

Since this manuscript was submitted for publication, the authors became aware of a similar extension of the Milner–Witten–Cates theory by Miklavic and Marcelja[23] through one of the referees. They treat the brush problem in the low potential regime and with low segment densities, which justifies using binary interactions for the nonelectrostatic potential. Miklavic and Marcelja obtain analytical expressions for segment densities, free energy, and interaction energy between two brushes; this affords a quick insight into the physics of a polyelectrolyte brush. However, the treatment of the problem in the low-potential, dilute solution regime requires low grafting densities and low chain lengths. In this regime, the mean-field approximation may not be strictly valid, since the coils may not overlap sufficiently. In any case, our approach would yield the same results as Miklavic and Marcelja's model in the low-potential, dilute segment concentration regime, since they define the total potential in a fashion similar to eq 10 and 13 (with ω replaced by $1 - 2\chi$ for low segment densities).

6. Conclusions

This work extends the SCF approach of Milner et al. for nonionic brushes to polyelectrolyte brushes. The theory is based on the observation that one of the results of Milner et al., namely, that the overall potential field acting on the segments is parabolic, remains valid even in the presence of electrostatic interactions among the charged segments and between the segments and the substrate. No a priori assumptions were made for the segment density profile, which resulted as a consequence of the SCF equations using the mean-field approximation. The approach followed is along the lines of the theories of Hesselink, Papenhuijzen et al., and Van der Schee and Lyklema for polyelectrolyte adsorption.

In contrast to the case of Milner et al., the computer segment density profiles are not parabolic due to the introduction of long-range electrostatic interactions, although the overall potential is. The present work, which is valid in the strong stretching limit[19] for polymer chains, also predicts that both the segment density distribution and the brush height are significantly affected by the brush charge, and the surface charge density plays no appreciable role. The substrate charge has little effect on the segment density distribution since in the limit of long and highly stretched chains (where this theory is valid) the Debye screening length is a small fraction of the overall brush height, over the range of practically encountered ionic strengths. However, the surface charge would be expected to play a significant role for shorter brushes and for highly compressed brushes, where the brush height becomes comparable to the Debye screening length.

As shown by Figure 1 and 2, both the brush charging and electrolyte concentration can affect the segment density profiles significantly. Since these parameters can be adjusted with relative ease by pH[5,6] or ionic strength, one has the means to "control" the brush configuration.

In the case of microporous membranes with grafted polyelectrolyte brushes within the pores, one would have a permanently altered membrane with particular properties depending on the polyelectrolyte molecule.

Experimental data on brush conformation are limited. Webber, Anderson, and Jhon[22] have performed a study on solvent flow through membranes with adsorbed diblock copolymers and measured the effect of solvent quality, molecular weight, etc., on the hydrodynamic thickness of the polymer layer. Hadziioannou et al. and Tauton et al.[20,21] have measured the forces between surfaces with adsorbed copolymers. These are some ways of probing the segment density in a brush. Direct measurements of segment density could be made by small-angle neutron scattering (SANS)[28-30] or evanescent wave induced fluorescence experiments.[31,32] As suggested by Milner et al., one could probe the end segment density distribution by fluorescent tagging of end segments and relate it to the total segment density distribution. This, as mentioned by them, would be a more robust test of the parabolic potential theory. Hydrodynamic thickness measurements can also be used,[33,34] as mentioned earlier, as indirect methods, although the detailed picture can only be obtained by SANS or fluorescent tagging.

Acknowledgment. We greatly appreciate various insightful and valuable discussions with Prof. C. G. Montgomery of the Department of Physics, The University of Toledo, and Noubar Tcheurekdjian of S. C. Johnson and Son Inc.

References and Notes

(1) Napper, D. H. *Polymeric Stabilization of Colloidal Dispersions*; Academic: London, 1983.
(2) Witten, T. A.; Pincus, P. A. *Macromolecules* **1986**, *19*, 2509.
(3) Scheutjens, J.; Fleer, G. J. *Macromolecules* **1985**, *18*, 1882.
(4) Hesselink, F. Th. *J. Colloid Interface Sci.* **1977**, *60*, 448.
(5) Pefferkorn, E.; Scmitt, A.; Varoqui, R. *Biopolymers* **1982**, *21*, 1451.
(6) Idol, W. K.; Anderson, J. L. *J. Membr. Sci.* **1986**, *28*, 269.
(7) Alexander, S. *J. Phys. (Les Ulis, Fr.)* **1977**, *38*, 983.
(8) de Gennes, P.-G. *Macromolecules* **1980**, *13*, 1069.
(9) de Gennes, P.-G. *Adv. Colloid Interface Sci.* **1987**, *27*, 189.
(10) Scheutjens, J. M. H. M.; Fleer, G. J. *J. Phys. Chem.* **1979**, *83*, 1619.
(11) Cosgrove, T.; Heath, T.; van Lent, B.; Leermakers, F.; Scheutjens, J. *Macromolecules* **1987**, *20*, 1692.
(12) Edwards, S. F. *Proc. Phys. Soc.* **1965**, *85*, 613.
(13) de Gennes, P.-G. *Rep. Prog. Phys.* **1969**, *32*, 187.
(14) Dolan, A. K.; Edwards, S. F. *Proc. R. Soc., London A* **1974**, *337*, 509.
(15) Dolan, A. K.; Edwards, S. F. *Proc. R. Soc., London A* **1975**, *343*, 427.
(16) Helfand, E. J. *J. Chem. Phys.* **1975**, *62*, 999.
(17) Jones, I. S.; Richmond, P. J. *J. Chem. Soc., Faraday Trans. 2* **1977**, *73*, 1062.
(18) Ploehn, H. J.; Russel, W. B.; Hall, C. K. *Macromolecules* **1988**, *21*, 1075.
(19) Milner, S. T.; Witten, T. A.; Cates, M. E. *Macromolecules* **1988**, *21*, 2610.
(20) Hadziioannou, G.; Patel, S.; Granick, S.; Tirrell, M. *J. Am. Chem. Soc.* **1986**, *108*, 2869.
(21) Tauton, H. J.; Toprakcioglu, C.; Fetters, L. J.; Klein, J. *Nature* **1988**, *332*, 712.
(22) Webber, R. M.; Anderson, J. L.; Jhon, M. S. in session on "Block Copolymers in Solutions and Interfaces", 62nd Colloid and Surface Science Symposium; June 19–22, 1988, University Park, PA.
(23) Miklavic, S. J.; Marcelja, S. *J. Phys. Chem.* **1988**, *92*, 6718.
(24) Papenhuijzen, J.; Van der Schee, H. A.; Fleer, G. J. *J. Colloid Interface Sci.* **1985**, *104*, 540.
(25) Van der Schee, H. A.; Lyklema, J. *J. Phys. Chem.* **1984**, *88*, 6661.
(26) Hoeve, C. A. J. *J. Polym. Sci.* **1970**, *C30*, 361.
(27) Roe, R. J. *J. Chem. Phys.* **1974**, *60*, 4192.
(28) Cosgrove, T.; Cohen Stuart, M. A.; Vincent, B. *Adv. Colloid Interface Sci.* **1986**, *24*, 143.
(29) Cosgrove, T.; Heath, T. G.; Ryan, K. in session on "Polymers at Interfaces", Annual AIChE meeting; Nov 15–20, 19878 New York.
(30) Auvray, L.; Cotton, J. P.*Macromolecules* **1987**, *20*, 202.
(31) Caucheteux, I.; Ausserre, D.; Hervet, H.; Rondelez, F. *Phys. Rev. Lett.* **1985**, *54*, 1948.
(32) Caucheteux, I.; Ausserre, D.; Hervet, H.; Rondelez, F. in session on "Polymers at Interfaces", Annual AIChE meeting, Nov 15–20, 1987, New York.
(33) Varoqui, R.; Dejardin, P. *J. Chem. Phys.* **1977**, *66*, 4395.
(34) Cohen Stuart, M. A.; Waajen, F. H. W. H.; Cosgrove, T.; Vincent, B.; Crowley, T. L. *Macromolecules* **1984**, *17*, 1825.

Poly[(aryloxy)phosphazenes] with Phenylphenoxy and Related Bulky Side Groups. Synthesis, Thermal Transition Behavior, and Optical Properties

Harry R. Allcock,* Michael N. Mang, and Alexa A. Dembek

Department of Chemistry, The Pennsylvania State University, University Park, Pennsylvania 16802

Kenneth J. Wynne

Chemistry Division, Office of Naval Research, Arlington, Virginia 22217.
Received November 29, 1988; Revised Manuscript Received March 31, 1989

ABSTRACT: The effect of steric hindrance on the synthesis of poly[(aryloxy)phosphazenes] that bear bulky aryloxy substituents is discussed. The syntheses of poly[(aryloxy)phosphazenes] with the general formula $[NP(OAr')_x(OAr'')_y]_n$, where OAr' and OAr'' are phenoxy, 2-methylphenoxy, 4-methylphenoxy, 2-phenylphenoxy, 3-phenylphenoxy, 4-phenylphenoxy, 4-benzylphenoxy, 4-cumylphenoxy, and 4-*tert*-butylphenoxy and $x + y = 2$, are described. These polymers were prepared by the interaction of the corresponding sodium aryloxide with poly(dichlorophosphazene) in dioxane at 150 °C in an autoclave. This procedure allows the synthesis of poly[(aryloxy)phosphazenes] with bulky side groups while avoiding equilibration depolymerization. The influence of side group structural parameters on the thermal transition behavior of the polymers is discussed. The refractive indices of the polymers were measured by using a modified critical angle method at $\lambda = 632$ nm and were found to vary between 1.561 and 1.686.

A wide variety of poly(organophosphazenes) has been prepared by the replacement of the chlorine atoms in soluble poly(dichlorophosphazene) by organic nucleophiles[1] such as amines, alkoxides, or aryl oxides.[2] The properties of these polymers vary widely depending on the structure of the organic substituents attached to the skeletal phos-

0024-9297/89/2222-4179$01.50/0